Journal of Energy Resources and Conversion
Volume 1 | Issue 1

Research Article Open Access

Determination of the Energy and Exergy of the Syngas Produced from Gasification of Rice Husk at Different Fluidization Velocities and Equivalence Ratios

Zhang Y[1], Ghaly A[*2], Mansaray K[3] and Li B[1]

[1]School of Energy Science and Engineering, Harbin Institute of Technology, Harbin, China
[2]Department of Process Engineering and Applied Science, Faculty of Engineering, Dalhousie University, Halifax, Canada
[3]Department of Mechanical and Maintenance Engineering, Fourah Bay College, Freetown, Sierra Leone

[*]**Corresponding author:** Ghaly A, Professor, Department of Process Engineering and Applied Science, Faculty of Engineering, Dalhousie University, Halifax, Nova Scotia, Canada, Tel: (902) 494-6014, E-mail: abdel.ghaly@dal.ca

Citation: Zhang Y, Ghaly A, Mansaray K, Li B (2019) Determination of the Energy and Exergy of the Syngas Produced from Gasification of Rice Husk at Different Fluidization Velocities and Equivalence Ratios. J Energ Res Convers 1(1): 104

Received Date: September 26, 2019 **Accepted Date:** June 02, 2021 **Published Date:** June 04, 2021

Abstract

The energy and exergy of syngas from the gasification of rice husk in a dual distributor type fluidized bed gasifier were evaluated at various fluidization velocities (0.22, 0.28 and 0.33 m/s) and equivalence ratios (0,25, 0.30 AND 0.35). The results showed that the energy values of CO, H_2, N_2, CO_2, CH_4, C_2H_4 and C_2H_6 varied within the ranges of 2736.20-4144.24, 617.48-945.08, 1064.06-1872.61, 351.80-721.33, 1082.64-1806.59, 994.82-1878.93 and 0.00-239.01 kJ/kg fuel, respectively. The overall energy distribution was CO>(N_2 & CH_4 & C_2H_4)>H_2>CO_2>C_2H_6. Increasing the fluidization velocity from 0.22 m/s to 0.33 m/s (50.00%) decreased the total energy of syngas by 21.21-44.42% depending on the equivalent ratio used. However, when the equivalent ratio was increased from 0.25 to 0.35 (40.00%), the total energy of syngas fluctuated within the range of 6.40-17.37% depending on the fluidization velocity used. The exergy values of CO, H_2, N_2, CO_2, CH_4, C_2H_4 and C_2H_6 varied within the ranges of 2451.80-3736.32, 469.50-718.03, 321.31-699.74, 266.33-547.11, 975.58-1630.75, 932.77-1766.71 and 0.00-222.37 kJ/kg fuel, respectively. The overall exergy distribution was CO>(CH_4 & C_2H_4)>(H_2 & N_2)>CO_2>C_2H_6. Increasing fluidization velocity from 0.22 m/s to 0.33 m/s (50.00%) decreased the exergy of syngas by 22.28-49.76% depending on the equivalent ratio used. However, when the equivalent ratio was increased from 0.25 to 0.35 (40.00%), the total exergy of syngas fluctuated in the range of 6.76-13.84% depending on the fluidization velocity used. The results showed that the exergy values of syngas were lower than their energy values because different gas components contributed differently to the energy and exergy (the physical exergy of gas components are lower than the corresponding physical energy and the chemical exergy of combustible gases are lower than the corresponding chemical energy). The effect of fluidization velocity on the total energy and exergy of syngas was much greater than that of the equivalent ratio. The highest values of energy (10343.26 kJ/kg fuel) and exergy (8598.47 kJ/kg fuel) of the syngas were obtained at the fluidization velocity of 0.22 m/s and equivalent ratio of 0.25.

Keywords: Gasification; Rice Husk; Fluidized Bed Gasifier; Fluidization Velocity; Equivalent Ratio; Syngas; Energy; Exergy

Introduction

Rice is a staple food for over half (3.62 billion people) of the world's population and about one-fifth (1.45 billion people) of the world's population is engaged in rice cultivation [1,2]. The global paddy rice production was estimated to be 751.00 million tonnes (500.70 million tonnes milled rice) in 2014 [3]. Cultivation of this paddy rice produced the largest amount of crop residues (250.30 million tonnes) in 2014 in the forms of rice husk and rice straw [3,4]. Rice husk and rice straw are abundantly available as a renewable biomass material that can be used as an energy source in biochemical and thermochemical conversion processes. Compared with biochemical methods (biogas, bio-alcohol and biohydrogen), thermochemical methods (gasification, combustion and pyrolysis) are much faster, have higher efficiency, less costly and less selective of feed stocks [5,6].

Among the thermochemical technologies for energy recovery from biomass, gasification is one of the most promising conversion processes for the production of second generation fuels [5]. The advantages of biomass gasification are: (a) minimum waste products, (b) lower gas emissions, (c) higher recycling rates and (d) higher energy efficiencies [7-10]. Gasification of biomass results in a gas mixture containing CO, H2, N2, CO2, H2O and some hydrocarbons (CH_4, C_2H_4 and C_2H_6). The generated gas commonly referred to as syngas, can be combusted in burners, boilers and internal combustion engines to produce heat, mechanical power and electricity. It can also be used to produce synthetic liquid fuels and lubricants as well as chemical commodities such as methanol and ammonia [9,11-14].

Energy content is an important property of objects and is measured in joule. Work and heat are two processes that can transfer a given amount of energy. The joule is amount of energy transferred to an object by mechanical work that moves the object one meter against a force of one Newton. Energy can be converted to different forms but cannot be created or disrobed.

Exergy is a combination property of a system and its environment because it depends on the state of both the system and environment. Therefore, exergy is defined as a measure of how a certain material deviate from a state of equilibrium with the environment [15]. The exergy of a system is the maximum useful work possible during a process that brings the system into equilibrium with the environment. The exergy of a system in equilibrium with the environment is zero. Exergy is neither a thermodynamic property of matter nor a thermodynamic potential of a system. Therefore, in contrast to energy, exergy can be destroyed when a process involves a temperature change. The exergy destruction of a cycle is the sum of the exergy destruction of the processes that compose that cycle [16,17].

Energy and exergy can be used to evaluate the quality and quantity of energy sources as well as for evaluating and improving the efficiency of energy resource use [18]. In gasification of biomass materials, the energy conversion process and the quality of the gas produced are affected by several factors including the type of gasification system, bed height, fluidization velocity and equivalence ratio [19]. The main objectives of this study were: (a) to investigate the energy and exergy of syngas produced from the gasification of rice husk in a dual-distributor fluidized bed gasifier at various fluidization velocities and equivalence ratios and (b) to detail the distributions of energy and exergy of syngas as affected by the fluidization velocity and equivalence ratio.

Energy and Exergy Analyses

Energy of Syngas

The total energy of a flow gas can be written as the sum of various energy of the flow gas as follows [20]:

$$En = En_{ki} + En_{po} + En_{ph} + En_{ch} \tag{1}$$

where:

En	is the total energy of the gas stream (kJ/kg)
En_{ki}	is the kinetic energy of the gas stream (kJ/kg)
En_{po}	is the potential energy of the gas stream (kJ/kg)
En_{ph}	is the physical (or sensible) energy of the gas stream (kJ/kg)
En_{ch}	is the chemical energy of the gas stream (kJ/kg)

Zhang *et al.* [21] reported that the kinetic energy and potential energy contributed very small portions (0.000001-0.0003% and 0.00002-0.003% of the total energy of the gases, respectively) of the total energy and can, therefore, be neglected. Equation (1) can, then, be simplified as follows:

$$En = En_{ph} + En_{ch} \tag{2}$$

The syngas generated from biomass gasification is a mixture of H_2, CO, CO_2, CH_4, C_2H_4, C_2H_6, N_2 and O_2. The physical energy of syngas can be calculated from the following linear mixing equation [22]:

$$En_{ph} = \sum_i n_i h_i \tag{3}$$

Where:

ni	is the molar yield of gas component *i* (mol/kg)
hi	is the specific enthalpy of gas component *i* (kJ/kmol)

Based on the specific enthalpy of gases at the environmental state specified in Table 1 (temperature T_0 =25 °C and pressure P_0 = 1 atm), the specific enthalpy of gases at arbitrary temperatures can be obtained from the following equation [23]:

$$h = h_0 + \int_{T_0}^{T} c_p \mathrm{d}T \tag{4}$$

Where:

h	is the specific enthalpy of gas component at the arbitrary temperature (kJ/kmol)
h_0	is the specific enthalpy of gas at the environmental state (kJ/kmol)
T_0	is the environmental temperature (298.15 K)
T	is the temperature of the gas under an arbitrary condition (K)
c_p	is the constant pressure specific heat capacity (kJ/kmol K)

The empirical equation of the constant pressure specific heat capacity is written as follows [23]:

$$\overline{c_p} = a + bT + cT^2 + dT^3 \tag{5}$$

Gas	HHV (kJ/kmol)[a]	ex_{ch} (kJ/kmol)[b]	h_0 (kJ/kmol)[a]	s_0 (kJ/kmol K)[a]
N_2	0	720	8669	191.502
O_2	0	3970	8682	205.033
H_2	285840	236100	8468	130.574
CO	282990	275100	8669	197.543
CO_2	0	19870	9364	213.685
CH_4	890360	831650	—	—
C_2H_4	1408400	1361100	—	—
C_2H_6	1556100	1495840	—	—

[a]Cengel and Boles [24]
[b]Moran *et al.* [25]

Table 1: Higher heating value (HHV), chemical exergy (ex_{ch}), specific enthalpy (h_0) and specific entropy (s_0) of some gases at standard temperature (25 °C) and pressure (1 atm)

Where:

a,b,c,d are the coefficients of constant pressure specific heat capacity (Table 2).

The chemical energy of syngas is expressed as follows [20]:

$$En_{ch} = \sum_i n_i HHV_i \tag{6}$$

Where:

HHV_i is the higher heating value of gas component *i* (kJ/kmol)

Exergy of Syngas

The total exergy of a flow gas can be written as the sum of various exergy of the flow gas as follows [26]:

$$Ex = Ex_{ki} + Ex_{po} + Ex_{ph} + Ex_{ch} \tag{7}$$

Where:

Ex is the total exergy of the gas stream (kJ/kg)

Ex_{ki} is the kinetic exergy of the gas stream (kJ/kg)
Ex_{po} is the potential exergy of the gas stream (kJ/kg)
Ex_{ph} is the physical exergy of the gas stream (kJ/kg)
Ex_{ch} is the chemical exergy of the gas stream (kJ/kg)

According to Zhang *et al.* [21], the kinetic exergy and potential exergy represent very small amounts (0.000002-0.007% and 0.00002-0.009% of the total exergy of the gases, respectively) of the total exergy and can, therefore, be neglected. Thus, equation (7) can then be simplified to the following equation:

$$Ex = Ex_{ph} + Ex_{ch} \tag{8}$$

Gas	*a*	*b* (×10⁻²)	*c* (×10⁻⁵)	*d* (×10⁻⁹)	Temperature Range (K)
N2	28.90	–0.157	0.808	–2.873	273–1800
O2	25.48	1.520	–0.716	1.312	273–1800
H2	29.11	–0.192	0.400	–0.870	273–1800
CO	28.16	0.168	0.533	–2.222	273–1800
CO2	22.26	5.981	–3.501	7.469	273–1800
CH4	19.89	5.024	1.269	–11.010	273–1500
C2H4	3.95	15.640	–8.344	17.670	273–1500
C2H6	6.90	17.270	–6.406	7.285	273–1500

Table 2: Coefficients of constant pressure specific heat capacity of some gases [24]

The physical exergy of syngas is calculated as follows [21]:

$$Ex_{ph} = \sum_i n_i \text{üühü}\ h_o \ -T_o \ s - s_o \tag{9}$$

Where:

s is the specific entropy of gas component i at the arbitrary temperature (kJ/kmol K)

s_0 is the specific entropy of gas component i at the environmental state (kJ/kmol K)

Based on the specific enthalpy of N_2, O_2, H_2, CO, CO_2, CH_4, C_2H_4 and C_2H_6 at the environmental state shown in Table 1, the specific entropy of gases at arbitrary temperatures can be obtained as follows [23]:

$$s = s_0 + \int_{T_0}^{T} \frac{c_p}{T} \mathrm{d}T - R\ln\frac{P}{P_0} \tag{10}$$

Where:

The chemical exergy of syngas is calculated as follows [21]:

$$s = s_0 + \int_{T_0}^{T} \frac{c_p}{T} \mathrm{d}T - R\ln\frac{P}{P_0} \tag{11}$$

Where:

ex_{ich} is the standard chemical exergy of gas component i as shown in Table 1 (kJ/kmol)

Materials and Methods

Rice Husks

Rice husk (Lemont LG) was obtained from Brousand Rice Mills, Louisiana, USA. The rice husk was a relatively uniform material and did not require any treatment before use. The properties of the rice husk are given in Table 3.

Alumina Sand

Alumina sand was used as inert bed material in the fluidized bed gasifier in order to avoid the agglomeration problems encountered in previous experiments with silica sand [27]. It was obtained from Diamonite Products Limited, Ohio, USA. The alumina sand used in this study was kiln fired at 1500 °C and very spherical in shape. The main characteristics and chemical composition of the alumina sand are given in Table 4.

Experimental Apparatus

Figure 1 shows a schematic of the fluidized bed gasification system used in this study. It consisted of a dual distributor fluidized bed gasifier, a gas sampling system and a computer and data acquisition system.

Characteristics	Value	Unit
Moisture content	9.08	%
Length range	2.0-10.8	mm
Width range	0.9-2.6	mm
Bulk density	92	kg/m^3
Lower heating value	14.22	MJ/kg
Proximate analysis [a]		
Volatile mater	66.40	%
Fixed carbon	13.60	%
Ash	20.00	%
Ultimate analysis [a]		
C	37.60	%
H	5.42	%
O	36.56	%
N	0.38	%
S	0.03	%
Cl	0.01	%
Ash	20.00	%

[a]Weight percentage on dry basis

Table 3: Some characteristics of the rice husk

The dual distributor fluidised bed gasifier is a further development of a spout-fluidized bed in which a bubbling fluidized bed is maintained at the outer region of the bed while the active spout is maintained at the center. The basic physical difference between the two is the presence of a secondary distributor plate above a secondary column to create the spout. By virtue of its design, the dual distributor fluidized bed ensures a uniform biomass distribution and a more homogeneous mixture of biomass and bed materials since the biomass is pneumatically introduced through the bottom center of the reactor from the secondary column and the spout entrains bed particles from the bottom of the bed, mixing them with biomass and secondary air and then transporting the mixture into the upper region of the bed as shown in Figure 2. The bed particles and the unreacted biomass proceed in a three-dimensional fashion by the movement of bubbles in the bed. The systematic pattern of solids movement gives rise to a unique hydrodynamic system which is more suitable for the gasification of low-density biomass materials compared to other conventional reactors.

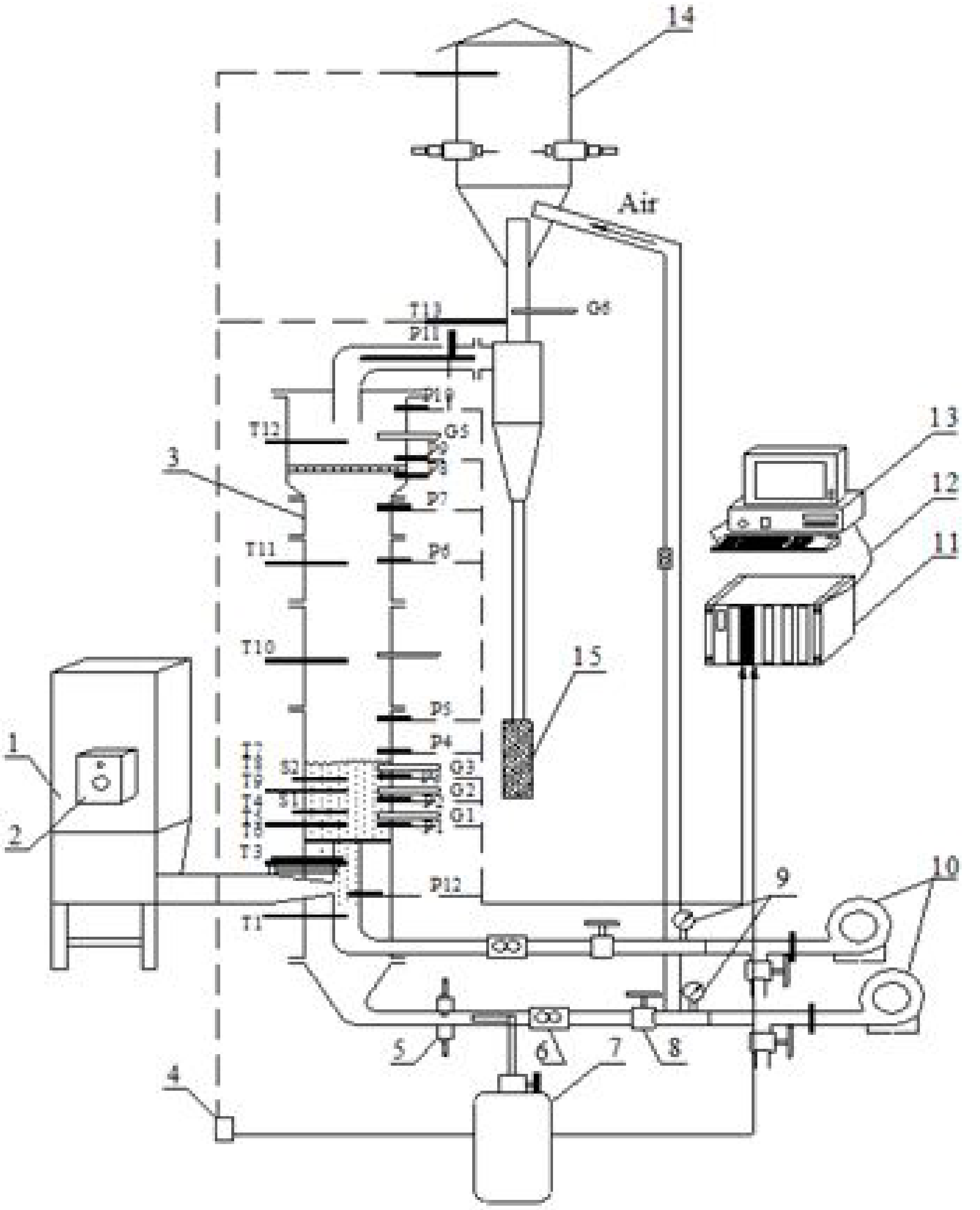

1-Feeder
2-Control Panel
3-De-entrainment Device
4-Ignition Electrodes
5-Torch
6-Flowmeters

7-Propane Tank
8-Main-Valves
9-Pressure Gauges
10-Blower
11-SCXI Data Acquisition
12-Parallel Port Cable

13-Computer
14-Afterburner
15-Ash Collector
P1-P12: Pressure Probes
T1-T14: Temperature Probes
G1-G6: Gas Sampling Probes
S1-S2: Solids Sampling Probes

Figure 1: Schematic diagram of the dual-distributor fluidized bed gasifier and associated equipment

Characteristics	Value	Unit
Particle density	3450	kg/m^3
Bulk density	2000	kg/m^3
Maximum particle size	500	µm
Mean particle size	380	µm
Minimum particle size	250	µm
Minimum fluidization velocity [a]	0.15	m/s
Chemical composition		
Alumina (Al_2O_3)	85.00-90.00	%
Silica (SiO_2)	8.00-10.00	%
Calcium oxide (CaO)	0.50-2.00	%
Magnesia (MgO)	0.50-1.50	%
Soda (Na_2O)	0.10-0.40	%
Iron Oxide (Fe_2O_3)	0.10-0.30	%
Titania (TiO_2)	0.05-0.15	%
Potasia (K_2O)	0.01-0.05	%

[a]Calculated for ambient conditions

Table 4: Main characteristics of the alumina sand

The fluidized bed gasifier was made of 8 mm thick, 310 stainless steel cylinders of 255 mm diameter and 2700 mm height. The primary air (for fluidization), the secondary air (for biomass feeding) and the air required for the afterburner were supplied by identical air supply units. Each unit consisted of a blower, a pressure gauge having a pressure range of 0-690 kPa, a main valve to control the air flow rate, a by-pass valve to prevent overheating of the electric motor, a steel pipe having an inner diameter of 50 mm and a flowmeter. The blower (Model ENGENAIR R4310A-2, Benton Harbour, Michigan, USA) is driven by a 4.8 hp (three-phase 220 volts and 13.4 amps) electric motor (Baldor Industrial Motor, Benton Harbour, Michigan, USA) and had a maximum flow capacity of 4.87 m3/min and maximum pressure of 20 kPa. Each blower inlet had a filter (with a micron rating of 25 and a maximum flow of 7.08 m3/min) to clean the incoming air of contaminants such as dust particles and water. Flow Cell Bypass flowmeters (Metal FLT-type, Cat. No. N-03251-60, Cole Parmar, Chicago, Illinois, USA) were used to measure the air supply rates. Each flowmeter was accurate to 2.5% of full scale and could be used up to maximum temperature and pressure of 60 ^{o}C and 1035 kPa, respectively.

An enlarged disengagement section mounted on the top of the main fluidization column was used to reduce the elutriation rate from the fluidized bed. The height of the enlarged section was 395 mm whereas the bottom and top diameters were 255 and 355 mm, respectively. The angle of inclination was 30o from the vertical axis. A de-entrainment device (Figure 3) was placed inside the disengagement section. It consisted of 16 triangular blades made of 310 stainless steel and inclined 300 to the horizontal. The distance from the top of the blade to the overlapping one was 61 mm. The diameter of the structure was 344.4 mm giving a clearance of 5.6 mm between the device and the wall of the disengagement section. The total open area of the structure on the horizontal plane was 714 mm. A cyclone was connected to the exit of the disengagement section to capture the solid particles (dust, ash and char) escaping from the bed. The fluidization column and cyclone were insulated using a flexible thermal blanket (Ins wool-HP Blanket, A. P. Green Industries Inc., New Mexico, Missouri, USA) to reduce heat loss from the system. The gas leaves the cyclone through a stainless-steel pipe of 150 mm inside diameter to the combustion chamber of an afterburner. The afterburner consisted of two ignition electrodes, an air supply unit, a mixing chamber, a combustion chamber and an exhaust duct.

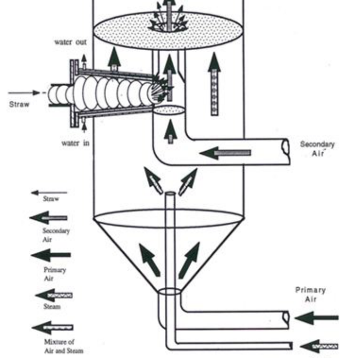

Figure 2: The air supplies and feeding mechanism

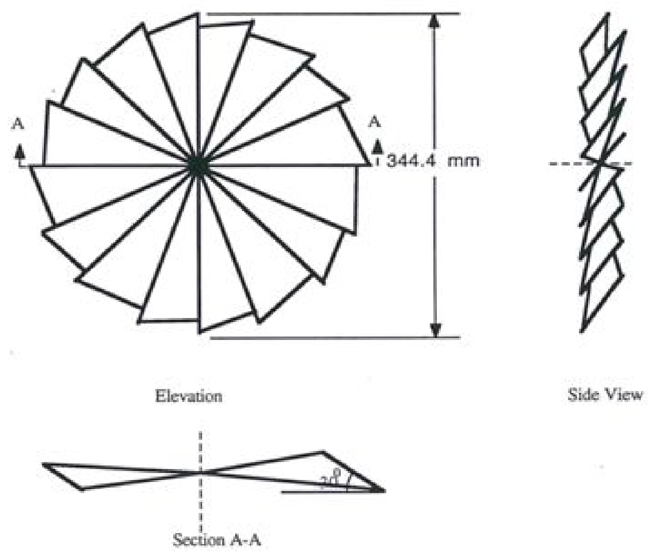

Figure 3: The de-entrainment device

The gas sampling system (Figure 4) consisted of a gas sampling probe, copper tubing, a three-way switch valve, a gas purifier, a compressed air line, a peristaltic pump, a sampling bulb, a pressure relief valve, a pressure gauge, a syringe and evacuated tubes. Stainless steel gas sampling probes (each with a cooling jacket) were used. Each probe was 12.5 mm in diameter and 500 mm in length. The diameter of the sampling tube placed inside the probe was 6.4 mm. Gas sampling probes were located within the bed, above the bed, in the enlarged section and at the exit of the cyclone. A pump (Master-Flex peristaltic pump, Cat. No. N-07567-70, Cole Parmer, Chicago, Illinois, USA) was used to draw the gas from the gasifier and compress it into the gas sampling bulb. The gas sampling bulbs (Cat. No. N-06650-40, Cole Parmer, Chicago, Illinois, USA) could store 0.25 L of gas sample at 100 kPa maximum gauge pressure. In order to maintain the gas pressure at the desired level inside the gas sampling bulbs, an adjustable relief valve (Cat. No. SS-4-CPA-3, Nupro Company, Willoughby, Ohio, USA) and a pressure gauge having a pressure range of 0-200 kPa (P0121BP, Invensys Systems, Inc., Houston, Texas, USA) were mounted at the exit of the gas sampling bulbs. A syringe and evacuated tube assembly were used to collect the gas sample from the gas sampling bulb. Vacutainer evacuated tubes having a volume of 10 mL each (Co. Model 6430, Becton Dickinson, Franklin Lakes, New Jersey, USA) were used to store the gas samples. These tubes were initially evacuated by the manufacturer up to 80% by volume. They were re-evacuated up to 99% by volume using a vacuum pump before being used. To remove moisture, tar and impurities from the gas, a gas purifier (Cat. No. N-01418-50, Cole Parmer, Chicago, Illinois, USA) was placed between the gas sampling bulb and the Master-Flex peristaltic pump.

A microcomputer (IBM compatible PC-2000 XT computer) and a data acquisition system were used to record and display the measured temperature values. An analog/digital conversion card (Cat. No. N-08109-25, Cole Parmer, Chicago, Illinois, USA) was used together with two thermocouple Amplifier-Multiplexers (Cat. No. N-08109-00, Cole Parmer, Chicago, Illinois, USA). The thermocouple Amplifier-Multiplexers (which each can read up to six thermocouples) provided cold-junction compensation and permitted resolution of thermocouple inputs up to ± 0.1 °C. The data logging software (Cat. No. N-08109-32, Cole Parmer, Chicago, Illinois, USA), which could read 16 inputs in one second, was modified and used to display the temperature and feed rate values on screen and store data in the computer.

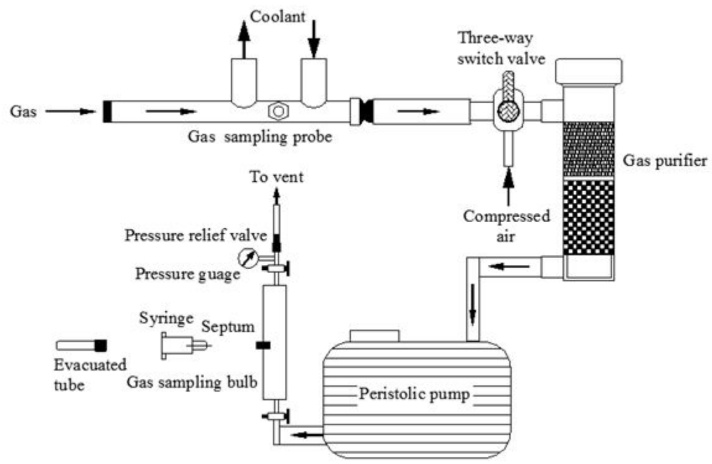

Figure 4: The gas sampling system

Experimental Procedure

The effects of fluidization velocity (0.22, 0.28 and 0.33 m/s) and equivalence ratio (0.25, 0.30 and 0.35) on the energy and exergy of syngas were investigated. The fluidization velocity (FV) was controlled by altering the primary air supply rate though the main distributor plate. The equivalence ratio (ER), defined as the ratio of actual air-fuel to stoichiometric air-fuel, was varied by varying the primary air supply rate though the main distributor plate. The flow rates of feedstock and air at various fluidization velocity-equivalence ratio combinations are given in Table 5.

A specially designed feeder for rice husk [28] was used to feed the biomass material into the gasifier. The feeder was filled with a known weight of rice husk. The alumina sand was placed into the reactor to a bed height of 25.5 cm. The primary air supply was turned on to fluidize the sand particles in the main fluidization column and the air flow rate was adjusted to 0.57 m^3/min. The temperature of the bed material was raised to 600 °C by combusting the propane-air mixture. The start-up system was then shut down while keeping the primary air supply on to cool the bottom section (wind-box) of the gasifier before starting to feed the rice husk. The computer-based data acquisition system was activated to monitor and record the temperature and feed rate values. When the temperature in the secondary column reached 600 °C, the secondary air supply was turned on and adjusted to the minimum rate (0.57 m^3/min) required to carry the sand particles from the secondary column into the main column. The feeder was turned on and the feed rate was adjusted to allow excess air in order to achieve complete combustion of rice husk. The bed temperature increased rapidly (to 750 °C) by the energy released from the combustion of rice husk.

The fuel feed rate and air flow rates were adjusted to the desired respective levels and the system was operated under this condition for half an hour to ensure that the steady state condition was reached in the fluidized bed. Gas samples were then collected during a period of 5 min. When sampling and data recording were completed, the feeder and the secondary and primary air supplies were shut down. The ash collector was replaced by an empty ash collector. The same procedure was followed at all fluidization velocity-equivalence ratio combinations.

FV (m/s)	ER	Rice Husk (kg/min)	Air (m^3/min)
0.22	0.30	0.56	0.84
	0.35	0.48	0.84
0.28	0.25	0.86	1.02
	0.30	0.72	1.02
	0.35	0.61	1.02
0.33	0.25	1.02	1.21
	0.30	0.85	1.21
	0.35	0.73	1.21

FV= the fluidization velocity
ER= the equivalence ratio
Table 5: Flow rates of rice husk and air

Gas Sampling and Analysis

The gas sampling procedure was initiated by purging the line and the gas sampling probe with compressed air (550 kPa). Using the three-way switch valve, the gas sampling probe was disconnected from the compressed air line and connected to the sampling line. The peristaltic pump was turned on to draw the gas from the gasifier through the gas sampling probe and compress it into the gas sampling bulb. The valve at the exit of the sampling bulb was kept open for three minutes in order to flush the sampling bulb with fresh gas from the gasifier. The valve was closed and the sampling bulb was filled with the gas sample. The gas sample was collected in an evacuated tube using a syringe. The tube was kept in position for about one minute to allow it to be filled with the gas from the sampling bulb. All the gases were analysed using a gas chromatograph (Hewlett Packard Model 5890 Series II Gas Chromatograph, GMI, Inc., Ramsey, Minnesota, USA). Argon was used as the carrier gas, so as to be able to detect hydrogen besides the other gas components.

Results and Discussion

Mean Temperatures of the Bed

The mean temperatures of the dense bed in the gasifier, where gasification reactions took place, at different fluidization velocities (FV) and equivalent ratios (ER) are shown in Table 6. The values are the average of 3 replicates.

When the fluidization velocity was increased from 0.22 to 0.33 (50.00%), the mean temperature increased from 665 °C to 700 °C (5.26%), from 744 °C to 766 °C (2.96%), and from 811 °C to 828 °C (2.10%) at the equivalent ratios of 0.25, 0.30, and 0.35, respectively. Sharma *et al*. [29] and Ergudenler and Ghaly [30] stated that higher fluidization velocity can breakdown segregated lumps and remove in-bed channels thereby resulting in a better particle mixing and higher temperatures. Mansaray *et al*. [31] stated that the increased air, resulting from the increase in fluidization velocity, increased the rate of exothermic reactions and raised the temperature of the bed. The results obtained from this study showed that higher fluidization velocity achieved a better mixing of feed biomass with bed material and thus resulted in better heat transfer and higher temperatures.

However, when the equivalent ratio was increased from 0.25 to 0.35 (40.00%), the mean temperature increased from 665°C to 811°C (21.95%), from 670 °C to 822 °C (22.69%), and from 700 °C to 828 °C (18.29%) for the FVs of 0.22, 0.28, and 0.33 m/s, respectively. Lickrastina *et al*. [32] stated that increasing equivalent ratio resulted in a faster gasification of biomass and a faster ignition of the volatiles with pronounced increase in the temperature to its peak value. Zhao *et al*. [33] stated that increase in equivalent ratio is favourable for the cracking reactions of heavy hydrocarbons which can also increase the gasification temperatures. The results obtained from this study showed that increasing equivalent ratio provided more air to the gasifier for biomass gasification and consequently resulted in faster ignition of the biomass and higher temperature.

The temperature range observed in this study (665-828 °C) is similar to those reported by Zhang *et al*. [19] and Ergudenler and Ghaly [30] for gasification of wheat straw (610-898 °C and 615-880 °C), that (665-835 °C) reported by Mansaray *et al*. [31] for gasification of rice husk and that (626-824 °C) reported by Khezri *et al*. [34] for gasification of Napier grass. In this study, the results also showed that the effect of equivalent ratio on the gasification temperature (18.29-22.69%) was much greater than that of fluidization velocity (2.10-5.26%).

Compositions of Syngas

Rice husk contain cellulose (50%), lignin (30%), ash (10%) and moisture (10%). The ash is about 92 % silica. The chemical formula for the organic content of the rice husk is $C_{40}H_{60}O_{0.5}N_{37}$ [35]. The products of the gasification reactions (Table 7) include CO, CO_2, H_2, CH_4 and H_2O. Also, some hydrocarbons such as C_2H_4 and C_2H_6 are produce. The syngas from air gasification may contain N from the gasifying air. The compositions of the syngas produced in this study at various fluidization velocities and equivalent ratios are shown in Table 6. The values are the average of 3 replicates. The CO, H_2, N_2, CO_2, CH_4, C_2H_4 and C_2H_6 varied within the ranges of 8.71-13.33, 1.98-3.00, 36.64-56.38, 8.60-15.15, 1.16-1.94, 0.68-1.29 and 0.00-0.15 mol/kg fuel, respectively.

The results showed that increasing the fluidization velocity decreased the yields of CO, H_2, CH_4, C_2H_4 and C_2H_6. Also increasing the fluidization velocity initially increased the yield of N_2 which then decreased with further increases in the fluidization velocity. However, the fluidization velocity showed no obvious effect on the yield of CO_2. Several researchers reported similar variations of gas components as a result of variations in the fluidization velocity. Mansaray *et al.* [31] stated that increasing fluidization velocity could increase the concentrations of N_2 and CO_2.

FV (m/s)	ER	Temperature (°C)	Gas Components (mol/kg fuel)							HHV (MJ/Nm³)
			CO	H_2	N_2	CO_2	CH_4	C_2H_4	C_2H_6	
0.22	0.25	665±5	13.33±0.66	2.68±0.13	37.88±1.89	9.68±0.69	1.94±0.09	1.29±0.06	0.15±0.00	5.03±0.15
	0.30	744±6	11.55±0.46	2.92±0.12	47.34±1.91	12.53±0.71	1.83±0.08	0.90±0.04	0.09±0.00	3.83±0.11
	0.35	811±6	11.27±0.52	3.00±0.13	56.21±2.01	15.15±0.77	1.75±0.07	0.96±0.04	0.04±0.00	3.28±0.11
0.28	0.25	670±5	12.17±0.58	2.51±0.10	39.55±1.99	9.65±0.71	1.57±0.07	0.94±0.05	0.14±0.00	4.38±0.12
	0.30	750±6	11.02±0.48	2.60±0.11	47.65±2.00	12.57±0.72	1.53±0.06	0.86±0.04	0.06±0.00	3.54±0.10
	0.35	822±7	10.99±0.46	2.87±0.12	56.38±2.02	15.15±0.74	1.63±0.07	0.92±0.05	0.00±0.00	3.15±0.09
0.33	0.25	700±5	8.78±0.41	1.98±0.09	36.64±1.87	8.60±0.69	1.16±0.05	0.78±0.04	0.09±0.00	3.75±0.09
	0.30	766±6	8.71±0.42	2.22±0.10	42.84±1.91	11.13±0.71	1.28±0.05	0.68±0.03	0.05±0.00	3.26±0.10
	0.35	828±7	9.33±0.44	2.47±0.10	48.73±1.94	13.22±0.72	1.40±0.04	0.74±0.03	0.00±0.00	3.09±0.08

FV= the fluidization velocity
ER= the equivalence ratio
HHV= the higher heating value of syngas
The values are the average of 3 samples ± standard deviation
Table 6: Bed temperature, gas composition and HHV

Reaction	Type of Reaction
(a) Combustion Reactions	
C + ½ O_2 <-> CO (1) C + O_2 <-> CO_2 (2) CO + ½ O_2 <-> CO_2 (3) H_2 + ½ O_2 <-> H_2O (4)	Partial oxidation Complete oxidation Complete oxidation Complete oxidation
(b) Heterogeneous Reactions	
C + H_2O <-> CO + H_2 (5) C +CO_2 <-> 2 CO (6) C + 2H_2 <-> CH_4 (7)	Water Reaction Boudouard Reaction Methanation
(c) Homogeneous Reactions	
CO + H_2O <-> CO_2 + H_2 (8) CH_4 +H_2O <-> CO + 3 H_2 (9)	Water gas shift Reaction Steam Methane reforming Reaction

Table 7: Gasification Reactions

Sadaka *et al.* [36] stated that increasing fluidization velocity could decrease the mole fractions of CO, H_2, CH_4, C_2H_4 and C_2H_6.

The results also showed that increasing the equivalent ratio increased the yields of H_2, N_2 and CO_2 and decreased the yield of C_2H_6. Also increasing the equivalent ratio initially decreased the yield of C_2H_4 which then increased with further increases in the equivalent ratio. However, the equivalent ratio showed no obvious effect on the yields of CO and C_2H_4. Yoon et al. [37] stated that increases in equivalent ratio can boost the oxidation reaction which supports the endothermic reactions (methanation, water gas shift and water gas reactions). Zhao *et al.* [33] stated that increase in equivalent ratio is favorable for the cracking reactions of heavy hydrocarbons. Ergudenler and Ghaly [30] reported that ER had a significant effect on the gas compositions.

HHV of Syngas

The HHVs of syngas produced at various fluidization velocities and equivalent ratios are shown in Table 6. The values are the average of 3 replicates

The results obtained from the present study showed that increasing the fluidization velocity from 0.22 to 0.33 (50.00%) decreased the mean HHVs of syngas from 5.03 to 3.75 (25.45%), from 3.83 to 3.26 (14.88%) and from 3.28 to 3.09 (5.79%) MJ/Nm^3 at the equivalent ratios of 0.25, 0.30 and 0.35, respectively. The results showed that increasing the fluidization velocity increased the amount of oxygen thereby increased the oxidation of combustible gases (reactions 2-4 in Table 7) and decreased the HHV of syngas. Similar results were reported by several authors. Mansaray *et al.* [31] stated that higher concentrations of products were caused by the increase of the air flow rate whereas lower HHV of syngas was obtained at higher fluidization velocity. Sadaka *et al.* [36] stated that increases in the fluidization velocity decreased the HHV of syngas as there were decreases in the combustible gases and increase in N_2.

When the equivalent ratio was increased from 0.25 to 0.35 (40.00%), the mean HHVs of syngas decreased from 5.03 to 3.28 (34.79%), from 4.38 to 3.15 (28.08%) and from 3.75 to 3.09 (17.60%) MJ/Nm^3 at the fluidization velocities of 0.22, 0.28 and 0.33 m/s, respectively. The results showed that lower equivalent ratio resulted in higher HHV and higher equivalent ratio decreased the combustible gases and reduced the HHV of syngas. Lickrastina *et al.* [32] stated that increases in equivalent ratio can enhance the transition from the heating/drying phase to the devolatilization phase, thus resulting in a faster gasification. Yoon *et al.* [37] stated that increases in equivalent ratio can boost the oxidation reaction which supports the endothermic reactions. However, Mansaray *et al.* [31], Yoon *et al.* [37] and Karmakar *et al.* [38] stated that higher equivalent ratio will decrease the concentrations of H_2 and CO and finally degrade the gas quality with more N_2 dilution and higher CO_2 generation due to the oxidization of larger fraction of carbon in feedstock.

The results obtained from this study showed that the effect of equivalent ratio (17.60-34.79%) on the HHV of syngas was more pronounced than that of fluidization velocity (5.79-25.45%). Ergudenler and Ghaly [30] and Mansrary *et al.* [31] also found that the fluidization velocity had lower effect on the HHV of the syngas compared to the equivalent ratio.

Energy Values of Syngas

The calculated energy values of gas components at various fluidization velocities and equivalent ratios are shown in Table 8 whereas the detailed energy distributions are shown in Table 9.

The energy values of CO, H_2, N_2, CO_2, CH_4, C_2H_4 and C_2H_6 varied from 2736.20 to 4144.24, from 617.48 to 945.08, from 1064.06 to 1872.61, from 351.80 to 721.33, from 1082.64 to 1806.59, from 994.82 to 1878.93 and from 0.00 to 239.01 kJ/kg fuel, respectively. Different gas components contributed differently to the total energy of syngas and the overall energy distribution of CO>(N_2, CH_4 & C_2H_4)>H_2>CO_2>C_2H_6 was observed. Equation (3) shows that the increases in enthalpy and yield of a gas can result in increases in the physical energy of the gas component. Also, equation (6) shows that the increase in yield of a gas can lead to increase in the chemical energy of gas. The effects of fluidization velocity and equivalent ratio on the total energy of syngas are shown in Figure 5. The decreases in the energy values were associated with the decreases in the yields of CO, H_2, CH_4, C_2H_4 and C_2H_6 .

When the fluidization velocity was increased from 0.22 to 0.33 (50.00%), the total energy of syngas decreased from 7161.78 to 10343.26 (44.42%), from 7555.05 to 9720.75 (28.67%) and from 8406.11 to 10188.65 (21.21%) kJ/kg fuel at the ERs of 0.25, 0.30 and 0.35, respectively. The results showed that when the equivalent ratio was increased from 0.25 to 0.35 (40.00%), the total energy of syngas varied from 9720.75 to 10343.26 (6.40%), from 9085.10 to 9870.39 (8.64%) and from 7161.77 to 8406.11 (17.37%) kJ/kg fuel for the fluidization velocities of 0.22, 0.28 and 0.33 m/s, respectively.

FV (m/s)	ER	Energy Values (kJ/kg fuel)						
		CO	H_2	N_2	CO_2	CH_4	C_2H_4	C_2H_6
0.22	0.25	4144.24	832.93	1064.06	377.51	1806.59	1878.93	239.01
	0.30	3620.70	914.78	1451.02	542.75	1713.05	1327.22	151.25
	0.35	3559.20	945.08	1846.41	711.95	1646.63	1421.39	58.00
0.28	0.25	3785.54	780.18	1117.33	378.89	1460.93	1371.07	226.71
	0.30	3456.54	813.78	1469.78	548.20	1429.56	1267.52	99.71
	0.35	3475.83	905.22	1872.61	721.33	1532.10	1363.31	0.00
0.33	0.25	2740.80	617.48	1070.50	351.80	1082.64	1147.51	151.04
	0.30	2736.20	698.13	1343.94	495.33	1199.07	994.82	87.57
	0.35	2950.93	779.21	1628.16	633.74	1315.61	1098.47	0.00

FV= the fluidization velocity
ER= the equivalence ratio
Table 8: Energy values of the gas components

FV (m/s)	ER	Energy Distribution
0.22	0.25	$CO>C_2H_4>CH_4>N_2>H_2>CO_2>C_2H_6$
	0.30	$CO>CH_4>N^2>C_2H_4>H_2>CO_2>C_2H_6$
	0.35	$CO>N_2>CH_4>C_2H_4>H_2>CO_2>C_2H_6$
0.28	0.25	$CO>CH_4>C_2H_4>N_2>H_2>CO_2>C_2H_6$
	0.30	$CO>N_2>CH_4>C_2H_4>H_2>CO_2>C_2H_6$
	0.35	$CO>N_2>CH_4>C_2H_4>H_2>CO_2>C_2H_6$
0.33	0.25	$CO>C_2H_4>CH_4>N_2>H_2>CO_2>C_2H_6$
	0.30	$CO>N_2>CH^4>C_2H_4>H_2>CO_2>C_2H_6$
	0.35	$CO>N_2>CH_4>C_2H_4>H_2>CO_2>C_2H_6$

Table 9: Energy distribution of syngas

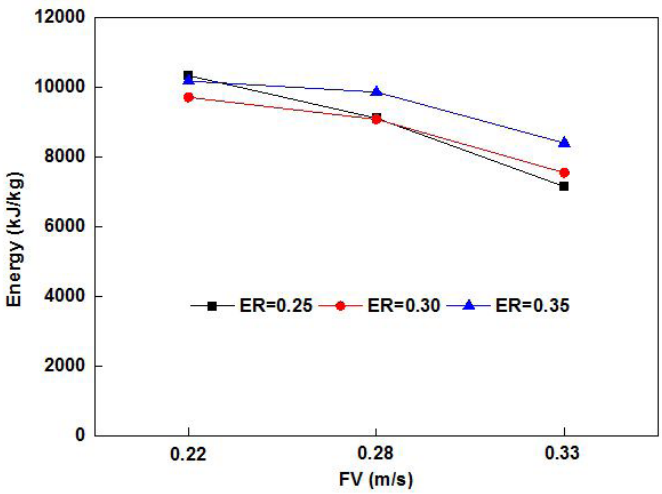

(**A**) Effect of FV

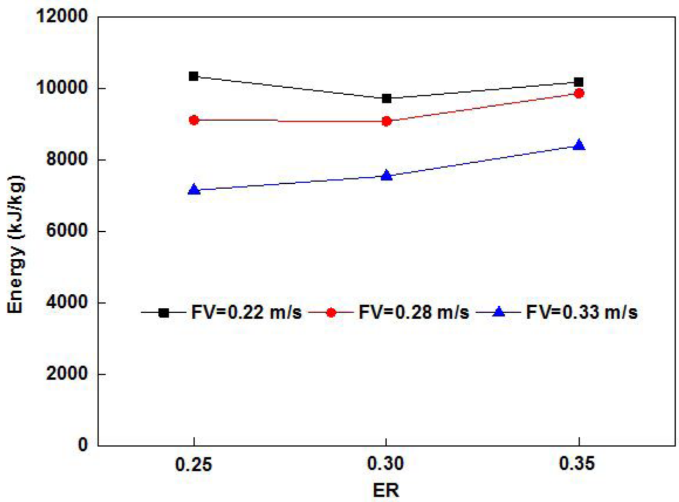

(**B**) Effect of ER

Figure 5: Effects of fluidization velocity and equivalent ratio on the energy value of syngas (**A**) Effect of FV; (**B**) Effect of ER

Sharma *et al.* [29] and Mansrary *et al.* [31] stated that fluidization velocity plays a key role in the gasification process and influences the gasifier performance in terms of gas composition and energy yield. Ergudenler and Ghaly [30], Mansaray *et al.* [31], Zhao *et al.* [33] and Sadaka *et a*l. [35] stated that equivalent ratio has significant effect on gas composition and energy yield.

The results obtained from this study showed that both the fluidization velocity and the equivalent ratio affected the gas composition and yield but effect of fluidization velocity on the total energy of syngas (21.21-44.42%) was much greater than that of equivalent ratio (6.40-17.37%). The highest energy (10343.26 kJ/kg fuel) of the syngas was achieved at the equivalent ratio of 0.25 and fluidization velocity of 0.22 m/s.

Exergy Values of Syngas

Table 10 shows the calculated exergy values of gas components at various fluidization velocities and equivalent ratios. The exergy values of CO, H_2, N_2, CO_2, CH_4, C_2H_4 and C_2H_6 varied from 2451.80 to 3736.32, from 469.50 to 718.03, from 321.31 to 699.74, from 266.33 to 547.11, from 975.58 to 1630.75, from 932.77 to 1766.71 and from 0.00 to 222.37 kJ/kg fuel, respectively.

Equation (9) shows that increases in enthalpy and entropy can result in increases in the physical exergy of gas component while the increase in the yield of gas component can lead to increases in the physical exergy. Equation (11) shows that increases in the yield of gas component can result in increases in its chemical exergy. The results showed that the exergy values of the gas components (Table10) were lower than their corresponding energy values (Table 8). This is because: (A) the physical exergy of a gas component is lower than the corresponding physical energy and (B) the chemical exergy values of combustible gases are lower than the corresponding chemical energy values (HHVs) as shown in Table 1. Similar results were reported by several authors [19,36,37] for syngas' obtained from gasification of various biomass fuels.

FV (m/s)	ER	Gas Components (mol/kg fuel)						
		CO	H_2	N_2	CO_2	CH_4	C_2H_4	C_2H_6
0.22	0.25	3736.32	634.57	321.31	286.45	1630.75	1766.71	222.37
	0.30	3249.94	696.06	495.20	412.01	1543.27	1245.20	140.37
	0.35	3185.74	718.03	681.60	540.10	1481.06	1331.99	53.67
0.28	0.25	3409.95	593.98	344.70	287.38	1317.81	1288.35	210.89
	0.30	3101.21	618.50	507.16	416.38	1287.11	1189.00	92.47
	0.35	3109.90	687.43	699.74	547.11	1377.53	1277.27	0.00
0.33	0.25	2462.91	469.50	349.19	266.33	975.58	1077.65	140.35
	0.30	2451.80	530.41	474.57	376.01	1079.15	932.77	81.19
	0.35	2639.56	591.70	612.02	480.91	1182.75	1028.93	0.00

FV= the fluidization velocity
ER= the equivalence ratio
Table 10: Exergy values of gas components

FV (m/s)	ER	Energy Distribution
0.22	0.25	$CO>C_2H_4>CH_4>H_2>N_2>CO_2>C_2H_6$
	0.30	$CO>CH_4>C_2H_4>H_2>N_2>CO_2>C_2H_6$
	0.35	$CO>CH_4>C_2H_4>H_2>N_2>CO_2>C^2H_6$
0.28	0.25	$CO>CH_4>C_2H_4>H_2>N_2>CO_2>C_2H_6$
	0.30	$CO>CH_4>C_2H_4>H_2>N_2>CO_2>C_2H_6$
	0.35	$CO>CH_4>C_2H_4>N_2>H_2>CO_2>C_2H_6$
0.33	0.25	$CO>C_2H_4>CH_4>H_2>N_2>CO_2>C_2H_6$
	0.30	$CO>CH_4>C_2H_4>H_2>N_2>CO_2>C_2H_6$
	0.35	$CO>CH_4>C_2H_4>N_2>H_2>CO_2>C_2H_6$

FV= the fluidization velocity
ER= the equivalence ratio
Table 11: Exergy distribution of syngas

Table 11 shows the detailed exergy distributions of gas components. Different gas components contributed differently to the total exergy of the syngas and the overall exergy distribution of $CO>(CH_4$ & $C_2H_4)>(H_2$ & $N_2)>CO_2>C_2H_6$ was observed. This is different from the energy distribution [$CO>(N_2$ & CH_4 & $C_2H_4)>H_2>CO_2>C_2H_6$] because different gases have different chemical energy/exergy ratios [25]. Zhang *et al.* [20] reported chemical/physical energy ratios of product gases in the range of 2.16-5.20 and chemical/physical exergy ratios the range of.

The effects of fluidization velocity and equivalent ratio on the total exergy of syngas are shown in Figure 6. The decreases in the exergy values were caused by the decreases in the yields of CO, H_2, N_2, CH_4, C_2H_4 and C_2H_6. When the fluidization velocity was increased from 0.22 to 0.33 (50.00%), the total exergy of the syngas decreased from 5741.52 to 8598.47 (49.76%), from 5925.91 to 7782.04 (31.32%) and from 6535.87 to 7992.19 (22.28%) kJ/kg fuel at the equivalent ratios of 0.25, 0.30 and 0.35, respectively [39].

When the equivalent ratio was increased from 0.25 to 0.35 (40.00%), the total exergy of the syngas varied in the ranges of 7782.04-8598.47 (10.49%), 7211.83-7698.99 (6.76%) and 5741.52-6535.87 (13.84%) kJ/kg fuel for the fluidization velocities of 0.22, 0.28 and 0.33 m/s, respectively. Sreejith *et al.* [40] and Prins *et al.* [41] stated that the energy and exergy contained in syngas exhibit maximum values at a critical equivalent ratio where all carbon in biomass fuel is consumed. Before reaching the optimum equivalent ratio, the energy and exergy of syngas increase when equivalent ratio is increased due to the conversion of solid carbon. However, beyond this maximum equivalent ratio, the energy and exergy decrease because the decreases in chemical energy and exergy are not fully compensated for by the increases in the physical energy and exergy. Zhang *et al.* [20] stated that the critical equivalent ratios is dependent on the composition of biomass fuel and different biomass fuels may have different critical equivalent ratios.

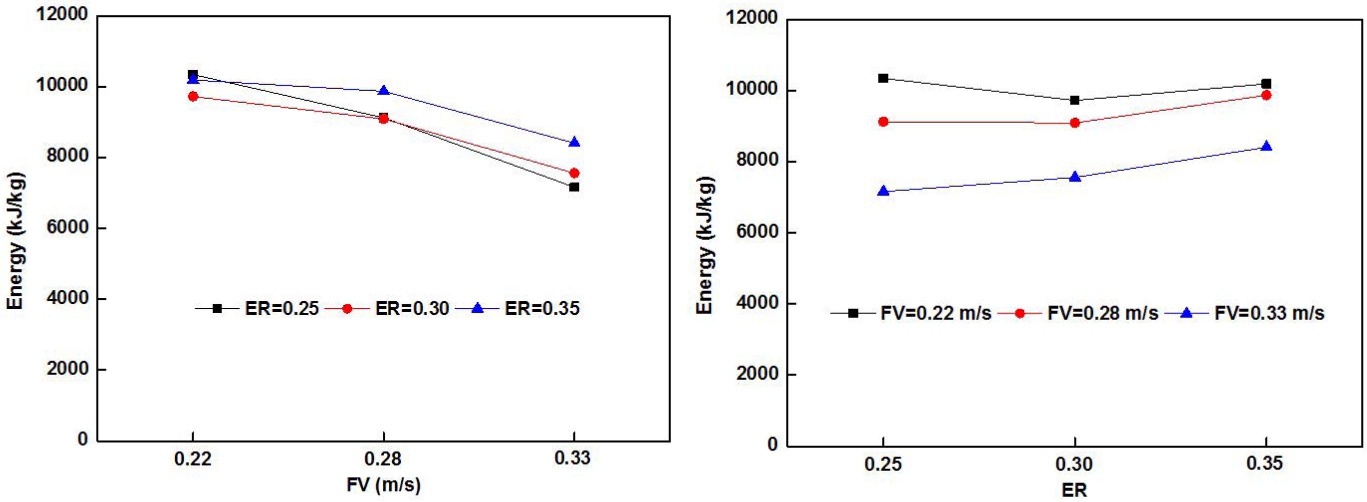

(**A**) Effect of FV (**B**) Effect of ER

Figure 6: Effects of fluidization velocity and equivalent ratio on the exergy value of syngas (**A**) Effect of FV; (**B**) Effect of ER

Zhang *et al.* [19] studied the energy and exergy of syngas produced from air-steam gasification of wheat straw in a dual-distributor fluidized bed gasifier under three fluidization velocities (0.35, 0.40 and 0.45 m/s), 3 steam flow rates (0.20, 0.25 and 0.30 kg/min) and 3 biomass: steam ratios (3.00, 4.00 and 5.00 kg/kg). The energy values of CO, H_2, N_2, CO_2, CH_4, C_2H_4 and C_2H_6 varied within the ranges of 1627.09-4646.60, 1543.30-2896.11, 274.75-1742.86, 82.03-574.24, 3225.39-4931.40, 1493.35-3777.44 and 892.74-2319.72 kJ/kg fuel, respectively. The overall energy distribution was (CH_4 & CO & C_2H_4 & H_2)>C_2H_6>(N_2 & CO_2). The results showed that when the fluidization velocity (FV) was increased from 0.35 m/s to 0.45 m/s (28.57%), the total energy of syngas increased by 1.16-28.59% and the total exergy of syngas increased by 1.45-26.93%, depending on the steam flow rate (SFR) and biomass: steam ratio (B:S) used.

The results obtained from this study showed that the effect of fluidization velocity on the total exergy of syngas (22.28-49.76%) was much greater than that of ER (6.76-13.84%). The highest exergy (8598.47 kJ/kg fuel) of the syngas were achieved at the equivalent ratio of 0.25 and fluidization velocity of 0.22 m/s.

Conclusions

The energy and exergy of syngas from the gasification of rice husk in a dual-distributor fluidized bed gasifier were evaluated at various fluidization velocities and equivalent ratios. The energy values of CO, H_2, N_2, CO_2, CH_4, C_2H_4 and C_2H_6 varied within the ranges of 2736.20-4144.24, 617.48-945.08, 1064.06-1872.61, 351.80-721.33, 1082.64-1806.59, 994.82-1878.93 and 0.00-239.01 kJ/kg fuel, respectively. The overall energy distribution was CO>(N_2 & CH_4 & C_2H_4)>H_2>CO_2>C_2H_6. The results showed that increasing the fluidization velocity from 0.22 to 0.33 (50.00%) decreased the total energy of syngas by 21.21-44.42% depending on the equivalent ratio used. However, when the equivalent ratio was increased from 0.25 to 0.35 (40.00%), the total energy of syngas fluctuated between 6.40% and 17.37% depending on the fluidization velocity used. The effect of fluidization velocity on the total energy of syngas was much greater than that of equivalent ratio. The exergy values of CO, H_2, N_2, CO_2, CH_4, C_2H_4 and C_2H_6 varied within the ranges of 2451.80-3736.32, 469.50-718.03, 321.31-699.74, 266.33-547.11, 975.58-1630.75, 932.77-1766.71 and 0.00-222.37 kJ/kg fuel, respectively. The overall exergy distribution was CO>(CH_4 & C_2H_4)>(H_2 & N_2)>CO_2>C_2H_6. Increasing the fluidization velocity from 0.22 to 0.33 (50.00%) decreased the exergy of syngas by 22.28-49.76% depending on the equivalent ratio used. However, when the equivalent ratio was increased from 0.25 to 0.35 (40.00%), the total exergy of syngas fluctuated between 6.76% and 13.84% depending on the fluidization velocity used. The effect of fluidization velocity on the total exergy of syngas was much greater than that of equivalent ratio. The results showed that the exergy values of syngas were lower than their energy values because various gas components contributed differently to the energy and exergy (the physical exergy of gas components are lower than the corresponding physical energy and the chemical exergy of combustible gases are lower than the corresponding chemical energy). The highest energy (10343.26 kJ/kg fuel) and exergy (8598.47 kJ/kg fuel) of syngas were obtained at the fluidization velocity of 0.22 m/s and equivalent ratio of 0.25.

The results obtained from this study showed that the effect of fluidization velocity on the total exergy of syngas (22.28-49.76%) was much greater than that of ER (6.76-13.84%). The highest exergy (8598.47 kJ/kg fuel) of the syngas were achieved at the equivalent ratio of 0.25.

Acknowledgements

The project was funded by National Science and Engineering Council (NSERC) of Canada. The support of China Postdoctoral Science Foundation is highly appreciated.

References

1. UN (2013) Department of Economic and Social Affairs, Population Division. United Nations, New York, USA.

2. Reidy S (2011) Global Rice Science Partnership seeks to increase productivity, improve efficiency of world staple crop, USA.

3. FAO (2014) Rice Market Monitor. Food and Agriculture Organization of the United Nations, Rome, Italy.

4. Soest PJV (2006) Rice straw, the role of silica and treatments to improve quality. Anim Feed Sci Technol 130: 137-71.

5. Parthasarathy P, Narayanan KS (2014) Hydrogen production from steam gasification of biomass: Influence of process parameters on hydrogen yield-A review. Renewable Energy 66: 570-9.

6. Balat H, Kırtay E (2010) Hydrogen from biomass - Present scenario and future prospects. Int J Hydrogen Energy 35: 7416-26.

7. Ruiz JA, Juárez MC, Morales MP, Muñoz P, Mendívil MA (2013) Biomass gasification for electricity generation: Review of current technology barriers. Renewable and Sustainable Energy Reviews 18: 174-83.

8. Materazzi M, Lettieri P, Mazzei L, Taylor R, Chapman C (2013) Thermodynamic modelling and evaluation of a two-stage thermal process for waste gasification. Fuel 108: 356-69.

9. Miguel GS, Domínguez MP, Hernández M, Sanz-Pérez F (2012) Characterization and potential applications of solid particles produced at a biomass gasification plant. Biomass and Bioenergy 47: 134-44.

10. Liu H, You L (1999) Characteristics and applications of the cold heat exergy of liquefied natural gas. Energy Conversion & Management 40: 1515-25.

11.Huang Z, He F, Zheng A, Zhao K, Chang S, et al. (2013) Synthesis gas production from biomass gasification using steam coupling with natural hematite as oxygen carrier. Energy 53: 244-51.

12. Pudasainee D, Paur H, Fleck S, Seifert H (2014) Trace metals emission in syngas from biomass gasification. Fuel Processing Technol 120: 54-60.

13. Brachi P, Chirone R, Miccio F, Miccio M, Picarelli A, et al. (2014) Fluidized bed co-gasification of biomass and polymeric wastes for a flexible end-use of the syngas: Focus on bio-methanol. Fuel 128: 88-98.

14. Hlina M, Hrabovsky M, Kavka T, Konrad M (2014) Production of high quality syngas from argon/water plasma gasification of biomass and waste. Waste Manag 34: 63-6.

15. Pierre P (1998) A to Z Thermodynamics. Oxford University Press, Oxford, UK.

16. Dincer I, Cengel YA (2001) Energy, entropy and exergy concepts and their role in thermal engineering. Entropy, 3: 116-49.

17. Bastianoni S, Fachini A, Susani L, Tiezzi E (2007) Energy as a function of exergy. Energy 32: 1158-62.

18. Zhang Y, Ghaly AE, Li B (2013) Determination of the exergy of four wheat straws. Am J Biochem and Biotechnol 9: 338-47.

19. Zhang Y, Ghaly AE, Sadaka S, Li B (2019) Determination of Energy and Exergy of Syngas produced from Air-steam Gasification of Wheat Straw in a Dual Distributer Fluidized Bed Gasifier. J Energy Research and Reviews 3:1-24 .

20. Zhang Y, Li B, Li H, Liu H (2011) Thermodynamic evaluation of biomass gasification with air in autothermal gasifiers. Thermochimica Acta 519: 65-71.

21. Zhang Y, Li B, Li H, Zhang B (2012) Exergy analysis of biomass utilization via steam gasification and partial oxidation. Thermochimica Acta 538: 21-8.

22. Loha C, Chattopadhyay H, Chatterjee PK (2011) Thermodynamic analysis of hydrogen rich synthetic gas generation from fluidized bed gasification of rice husk. Energy 36: 4063-71.

23. Lu Y, Guo L, Zhang X, Yan Q (2007) Thermodynamic modeling and analysis of biomass gasification for hydrogen production in supercritical water. Chem Eng J 131: 233-44.

24. Cengel YA, Boles MA (2006) Thermodynamics: an engineering approach (5th edn). McGraw-Hill, New York, USA

25. Moran MJ, Shapiro HN, Boettner DD, Bailey MB (2011) Fundamentals of engineering thermodynamics (7th Edn). John Wiley &Sons, Hoboken, New Jersey, USA.

26. Al-Weshahi MD, Anderson A, Tian G (2013) Exergy efficiency enhancement of MSF desalination by heat recovery from hot distillate water stages. Appl Therm Eng 53: 226-33.

27. Mansaray KG, Ghaly AE (1998) Agglomeration characteristics of silica sand-rice husk ash at elevated temperature. Energy Sources 20: 631-52.

28. Ghaly AE, Ergudenler A, AlSuhaibani S, Ramakrishnan V (2013) Development and evaluation of a lowdensity biomass feeding system for fluidized bed gasifer. Am J Eng and Appl Sci 6: 327-39.

29. Sharma AM, Kumar A, Patil KN, Huhnke RL (2013) Fluidization characteristics of a mixture of gasifier solid residues, switchgrass and inert material. Powder Technol 235: 661-8.

30. Ergudenler A, Ghaly AE (1992) Quality of gas produced from wheat straw in a dual-distributor type fluidized bed gasifier. Biomass and Bioenergy 3: 419-30.

31. Mansaray KG, Ghaly AE, Al-Taweel AM, Hamdullahpur F, Ugursal VI (1999) Air gasification of rice husk in a dual distributor type fluidized bed gasifier. Biomass and Bioenergy 17: 315-32.

32. Lickrastina A, Barmina I, Suzdalenko V, Zake M (2011) Gasification of pelletized renewable fuel for clean energy production. Fuel 90: 3352-8.

33. Zhao Y, Sun S, Che H, Guo Y, Gao C (2012) Characteristics of cyclone gasification of rice husk. Int J Hydrogen Energy 37: 16962-6.

34. Khezri R, Ghani WA, Biak DRA (2019) Experimental evaluation of Napier grass gasification in an autothermal bubbling fluidized bed reactor. Energies 12: 1617-538.

35. Mansaray KG, Ghaly AE (1997) Physical and thermochemical properties of rice husk. Energy Sources 19: 989-1004.

36. Sadaka SS, Ghaly AE, Sabbah MA (2002) Two phase biomass air-steam gasification model for fluidized bed reactors: Part II—model sensitivity. Biomass and Bioenergy 22: 463-77.

37. Yoon SJ, Son YI, Kim YK, Lee JG (2012) Gasification and power generation characteristics of rice husk and rice husk pellet using a downdraft fixed-bed gasifier. Renewable Energy 42: 163-7.

38. Karmakar MK, Mandal J, Haldar S, Chatterjee PK (2013) Investigation of fuel gas generation in a pilot scale fluidized bed autothermal gasifier using rice husk. Fuel 111: 584-91.

39. Karamarkovic R, Karamarkovic V (2010) Energy and exergy analysis of biomass gasification at different temperatures. Energy 35: 537-49.

40. Sreejith CC, Muraleedharan C, Arun P (2013) Energy and exergy analysis of steam gasification of biomass materials: a comparative study. Int J Ambient Energy 34: 35-52.

41. Prins MJ, Ptasinski KJ, Janssen FJJG (2003) Thermodynamics of gas-char reactions: first and second law analysis. Chem Eng Sci 58: 1003-11.